

論文 / 著書情報
Article / Book Information

Title	Influence of bond on the fatigue behavior of reinforced concrete beams without stirrups
Authors	B. Suryanto, N. Chijiwa
Citation	Proceedings of 10th International Conference on Bridge Maintenance, Safety and Management, , , pp. 2705-2710
Pub. date	2021, 4
DOI	https://doi.org/10.1201/9780429279119-369
Note	This is an Accepted Manuscript of a book chapter published by Routledge/CRC Press in Proceedings of 10th International Conference on Bridge Maintenance, Safety and Management, on 2021, 4, available online: http://dx.doi.org/10.1201/9780429279119-369

Influence of bond on the fatigue behavior of reinforced concrete beams without stirrups

B. Suryanto

Heriot-Watt University, Edinburgh, United Kingdom

N. Chijiwa

Tokyo Institute of Technology, Tokyo, Japan

ABSTRACT: This paper demonstrates the application of nonlinear finite element analysis for studying the behavior of shear-critical reinforced concrete beams with fully and non-bonded longitudinal reinforcement under monotonic and fatigue loading. The analysis platform employed has a built-in direct-path integration scheme which enables the simulation of high cycle fatigue problems. Nonlinear behavior of concrete under repetitive loading is represented by the integration of time-dependent and fatigue constitutive models using the multi-directional fixed-crack approach. The simulation results show that the nature of concrete cracking in the two beams is highly influenced by the bond between concrete and reinforcement. The removal of bond is shown to result in an enhancement in load capacity and deformability, which confirms the experimental evidence. When subjected to fatigue, however, the beam with non-bonded reinforcement is shown to display a significant increase in displacement amplitude and a reduction in fatigue life. A comparable fatigue life to the beam with conventional reinforcement is achieved when the enhancement in load capacity is not considered.

1 INTRODUCTION

The bond between concrete and steel reinforcement is one of key parameters of reinforced concrete. It affects several aspects of structural response such as tension stiffening, which influences crack spacing, crack width and overall deflection. It also affects internal load mechanisms which in turn affect the location and orientation of cracking, stress transfer across cracks, load capacity and overall ductility.

During the lifespan of a structure, bond deterioration can occur as a result of, for example, corrosion of steel reinforcement and this can have either a positive or negative influence on structural performance. Figure 1 displays the influence of damage (i.e. bond deterioration) on the shear capacity of reinforced concrete beam without transverse reinforcement. It is interesting to note from one of the test cases that damage can result in an enhancement in load capacity. As shown in Fig. 1, however, it is of importance to ensure that the anchorage of the bars at the support must remain fully intact as a brittle failure can otherwise result at a load significantly lower than the expected value (Chijiwa *et al.* 2011).

Apart from possible enhancement in load capacity, Ikeda and Uji (1980) were amongst the first to demonstrate that bond deterioration has also the potential to alter the mode of failure of shear critical beams. This was confirmed more recently by Kotsovos *et al.* (2015) who found that by removing

the bond between concrete and reinforcement, premature shear failure in concrete beam can possibly be either delayed or prevented.

This study presents the results of a numerical investigation into the response of two beams tested recently by Kotsovos *et al.* (2015). It aims to provide the mechanisms underlying the response observed at the structural level and extend the scope of the original experimental study through the investigation of the impact of bond removal under repetitive loading.

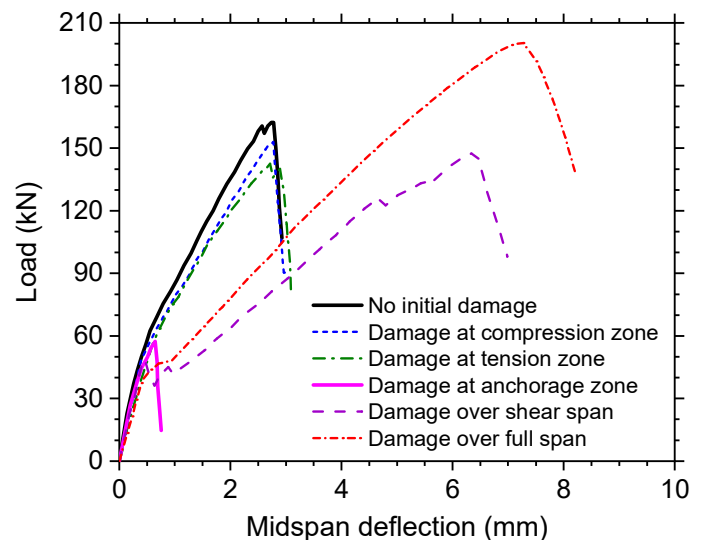


Figure 1. Influence of bond deterioration on the shear response of RC beams (Toongoenthong & Mackawa, 2005).

2 FINITE ELEMENT MODELING

2.1 Beam geometry and finite element meshes

Figure 2a displays the longitudinal profile and cross-sectional details of one of the two series of beams tested by Kotsovos *et al.* (2015). All beams were of rectangular cross section with the same width (150 mm) and overall depth (300 mm). The beams were reinforced with three 16 mm longitudinal reinforcement, and all were positioned at an effective depth of 270 mm and welded to steel plates at both ends of the beam to avoid premature anchorage failure. Here, only two beams were simulated: the control beam which had conventional reinforcement and the beam which had the main reinforcement *fully* unbonded throughout their length.

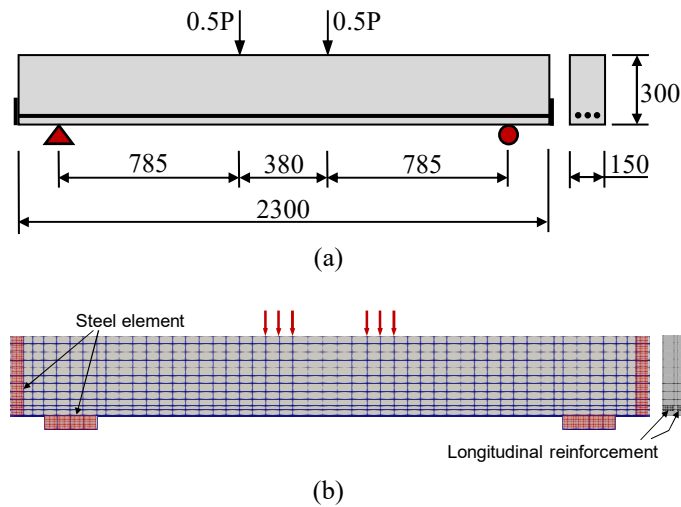


Figure 2. (a) Elevation details of the test beam; (b) finite element mesh used in the analysis.

The two beams were modeled using a mesh of 2300 four-node cubical elements (see Fig. 2b). Due to symmetry, only half width of the beam was modelled. In the longitudinal direction, however, it was considered appropriate to model the whole beam length to gain insights into the full behavior of the beam. The bottom reinforcement was modelled using the steel element, with the centroids of each element aligned with the centroids of the actual steel. The steel loading plates were not directly modelled. Instead, the applied load was modeled as nodal forces over two elements long. This was specifically done to enable future numerical investigations into the behavior of the beams under moving load. The support plates were modeled using steel elements, as shown in shaded in Fig. 2b. To avoid bond failure, particularly in the beam with non-bonded reinforcement, the anchor steel plates, which were welded to the reinforcement in the experiment, were specifically included in the FE representation at both ends of the beam using steel elements placed across the beam depth (see the shaded areas at both ends of the beam in Fig. 2b).

2.2 Analysis framework

To enable simulations of high-cycle fatigue problem, the nonlinear finite element analysis framework developed at the University of Tokyo, COM3, is used. It employs the direct-path integration scheme (Maekawa *et al.*, 2006a) and incorporates three primary constitutive models (Maekawa *et al.*, 2006b): compression, tension, and shear-transfer models, all of which are integrated using the multi-directional fixed-crack approach to produce the 3D behavior of cracked concrete under general loading conditions.

Figures 3a and b present the summary of multi-directional fixed-crack approach used to integrate the three constitutive models displayed in Figure 4 (Fujiyama & Maekawa, 2011). In these models, the cyclic damaging effect is considered as incremental plasticity and damage. In the compression model, for example, the fracture parameter K_c is introduced to consider both time-dependent incremental plasticity and fatigue damage progression. In the tension model, the tensile fracture parameter K_T is considered to account for path-dependent instantaneous fracture, time-dependent creep and incremental damage accumulation due to fatigue loading. Finally, the damage parameter X is incorporated by Gebreyouhannes *et al.* (2008) into the original contact density crack shear-transfer model of Li and Maekawa (1989) to represent progressive shear deterioration along crack interfaces. For more details, one should refer to Maekawa *et al.* (2008).

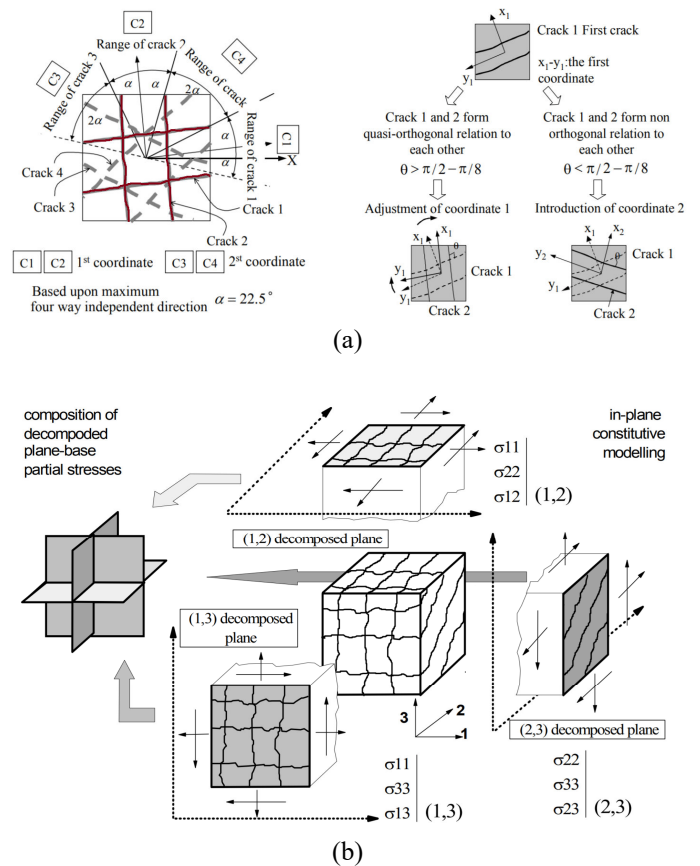


Figure 3. (a) Multi-directional fixed-crack approach and (b) 3D implementation of the concept (Maekawa *et al.*, 2003).

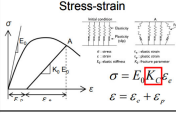
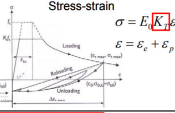
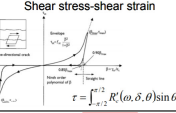
	Compression model	Tension model	Crack shear model
Core Constitutive law	 <p>Stress-strain</p> $\sigma = E_c \epsilon_c$ $\epsilon_c = \epsilon_e + \epsilon_p$	 <p>Stress-strain</p> $\sigma = E_c \epsilon_c$ $\epsilon_c = \epsilon_e + \epsilon_p$	 <p>Shear stress-shear strain</p>
Enhanced model for High cycle fatigue	<p>Fracture parameter K_{fc} considers time dependent plasticity & fracturing and cyclic fatigue damage</p> $dK_{fc} = \left(\frac{\partial K_{fc}}{\partial \epsilon_p} \right) d\epsilon_p + \left(\frac{\partial K_{fc}}{\partial \epsilon_e} \right) d\epsilon_e$ <p>time dependent cyclic fatigue</p> $\left(\frac{\partial K_{fc}}{\partial \epsilon_e} \right) - \lambda - \text{when } F_1 = 0$ $\left(\frac{\partial K_{fc}}{\partial \epsilon_e} \right) = - \left(\frac{\partial F_1}{\partial \epsilon_e} \right) \left(\frac{\partial F_1}{\partial \epsilon_e} \right) + \lambda - \text{when } F_1 = 0$ $\lambda = K' \left(1 - K' \right) \epsilon_e \cdot R$ <p>Maekawa and Maekawa 2004</p>	<p>Fracture parameter K_{ft} considers time dependent fracturing and cyclic fatigue damage</p> $dK_{ft} = F_1 dt + G d\epsilon_e + H d\epsilon_p$ <p>Time dependent fracturing</p> <p>Cyclic fatigue damage</p> <p>Maekawa et al. 2003, Hasegawa 2005</p>	<p>Accumulated path function X reduce shear associated with cyclic fatigue damage</p> $\tau = \frac{X}{\tau_0} \tau_0(\delta, \omega)$ $X = 1 - \frac{1}{10} \log_{10} \left(1 + \int d(\delta/\omega) \right) \geq 0.1$ <p>Contact density model by Li & Maekawa 1989</p> <p>Modification of accumulated path function by Gebreyohannes 2006</p>
Physical meaning	Decrease of stiffness and plasticity accumulation by continuous fracturing of concrete	Decrease of tension stiffness by bond fatigue	Decrease of shear transfer normal to crack by continuous deterioration of rough crack surface

Figure 4. Constitutive laws for cracked reinforced concrete in compression, tension and shear (Maekawa *et al.*, 2008; Fujiyama & Maekawa, 2011; and Hung *et al.*, 2019).

2.3 Material properties

The concrete and reinforcement material properties used in the analysis were as reported in the original publication, except for the tensile strength of concrete which was estimated from the compressive strength ($= 28$ MPa). The tensile strength of concrete in Beam 1 with conventional (fully bonded) longitudinal reinforcement was taken as 1.48 MPa ($= 70\%$ of the default value), in order to take into account initial shrinkage-induced stresses in the concrete due to restraining effect from the steel reinforcement. In Beam 2 with non-bonded longitudinal reinforcement, this was taken as 2.12 MPa (the default value). Furthermore, the compressive strength of the concrete in Beam 2 was increased by 20% to 33.7 MPa to consider the enhancement in strength due to additional confinement resulting from the restraining effects of the steel loading plate. The yield strength of the longitudinal reinforcement was taken as a constant value of 575 MPa.

To accurately model the non-bonded reinforcement in Beam 2, bond interface elements (Maekawa *et al.*, 2008) were incorporated between the smeared reinforcement elements and the surrounding concrete elements. The normal and shear stiffnesses in the closure mode were taken as 20 kN/mm and 1 kN/mm, respectively, whereas the corresponding stiffnesses in the opening mode were taken as zero. The frictional coefficient was taken as 0.3.

2.4 Finite element analysis

Each beam was subjected to both monotonic and fixed pulsating (fatigue) loads, with the load applied at the two locations on top under load control. In the monotonic loading analysis, the load was increased in 1 kN increment until failure, whereas in the fixed pulsating analysis, the load was cycled at a constant amplitude, which in this study, was taken at 70% of the numerically simulated peak load under static loading. The load was then cycled at a constant frequency of 1Hz.

3 SIMULATION RESULTS AND DISCUSSION

3.1 Response under monotonic loading

The load-deflection responses obtained from the nonlinear finite element analyses are compared to experimental data in Figure 5, with the corresponding crack patterns at failure and the predicted principal strain plots at intermediate and final stages of loading presented in Figures 6a and b for completeness. In general, reasonably accurate predictions of load-deflection response, mode of failure, crack pattern and location of failure are obtained.

The response of Beam 1 at intermediate stages of loading can generally be described as shear-flexure in nature (see, for example, Fig. 6a). It is predicted that Beam 1 fails in a brittle manner due to a sudden formation and propagation of a diagonal shear crack, which leads to a sudden loss in load carrying capacity (see Fig. 5). Prior to failure, the beam exhibits a limited measure of deformation, with the deflection at the peak load being less than one six hundredth of the span. Both analysis and experiment show that at ultimate, the critical crack propagates upwards and downwards rapidly, forming a typical S-shape failure crack pattern (see Fig. 6a) which is well documented (see, for example, Collins *et al.*, 2008; Bugalia & Maekawa, 2017; Saifullah *et al.*, 2017; Suryanto *et al.*, 2017; Suryanto & Staniforth 2019).

Unlike Beam 1, Beam 2 with non-bonded reinforcement is predicted to exhibit a more localised response over the center span, as shown by the two bands of principal strains in Fig. 6b. Confirming the experimental finding, the analysis also shows that by removing the bond between the concrete and the steel, premature shear failure can be avoided and as such, Beam 2 is able to reach a peak load which is twice that of Beam 1. This strength enhancement is in general agreement with test observations by Satoh *et al.* (2003); Matsuo *et al.* (2004); Toongoenthong & Maekawa (2005); and Yamada *et al.* (2018).

Apart from the enhancement in load capacity, the bond removal in Beam 2 results in a significant reduction in post-cracking stiffness which, in turn, increases the beam deflection at peak load, which is four times more than that of Beam 1. Moreover, it is evident that the complete bond removal has altered load carrying mechanism of the beam, from being a primarily beam action in Beam 1 to being a primarily tie and arch action in Beam 2.

With reference to Figure 4b, it is predicted that the failure of Beam 2 occurs shortly after the crushing of concrete in the compression zone over the center span. This failure then triggers sudden formation of inclined cracking and immediate horizontal splitting along the tension reinforcement, which are in good agreement with test observations. From the analysis, it is noted that accurate modelling of the bond between the concrete and the steel is important and has a direct impact on mode of failure.

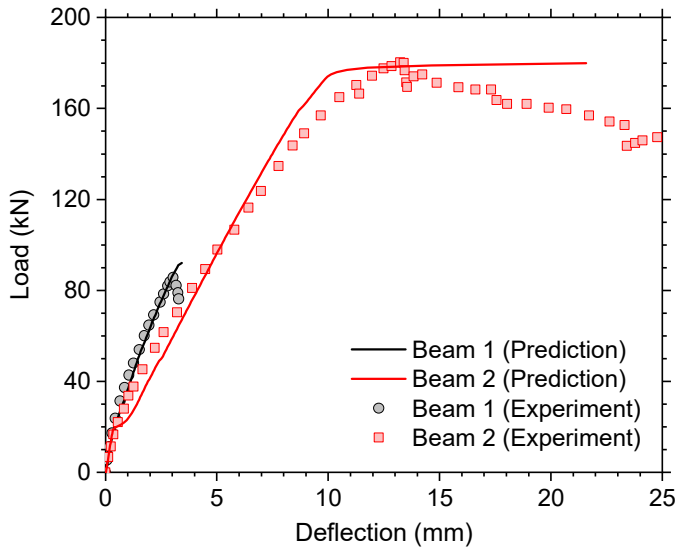


Figure 5. Predicted and observed load-deflection responses.

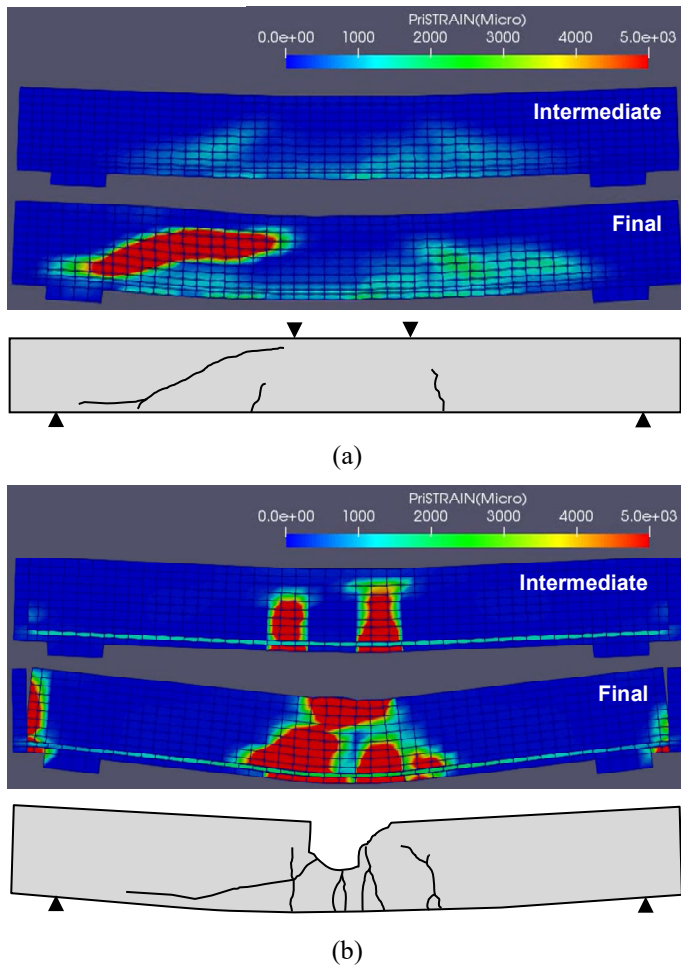


Figure 6. Maximum principal strain contours and failure crack patterns (Kotsovos *et al.*, 2015) for (a) Beam 1 and (b) Beam 2.

Although the removal of bond under static loading is appealing in terms of preventing premature shear failure, an in-depth understanding of the impact of bond removal under a more realistic loading condition is required. In a real-life situation, bond deterioration occurs mainly due to corrosion of the reinforcing steel, which is non-uniform and progressive (Biswas *et al.*, 2020). It may also cause the concrete to crack, which could help to dissipate stresses and prolong fatigue life (Maekawa *et al.*, 2006a).

3.2 Response under fatigue loading

Figure 7 presents the progress of beam deflection under a fixed-pulsating fatigue loading plotted against the logarithm of the number of cycles. For clarity, the principal tensile strain plots obtained at the first and final cycles of loading are presented in Figures 8a, b and c. Three analysis cases were run:

- Cases 1 and 2 in which the maximum applied load was fixed at 70% of the static load capacity, and
- Case 3 in which the maximum applied load was set at 70% of the predicted load capacity of the control beam (Beam 1).

It is apparent from Figure 7 that there is a steady increase in beam deflection with increasing number of cycles, particularly in Beam 1 with fully bonded tension reinforcement (Case 1). This would indicate that damage in the beam is progressive and accumulative, and the extent of which increases with increasing number of load cycles. At 70% of the load capacity, Beam 1 displays a fatigue life of approximately 60k cycles which is in excellent agreement with the fatigue life predicted using the equation proposed by Ueda and Okamura in 1982 and the findings reported by Gebreyouhannes *et al.*, 2008.

It is also evident from Figure 7 that by removing the bond between the concrete and reinforcement (Beam 2, Case 2), the displacement amplitude at the initial stages of loading increases significantly (approximately fivefold, from ~1.5 mm in Beam 1 to over 6 mm in Beam 2). This is mainly attributed to a substantial loss of stiffness after cracking, due to the complete removal of bond between concrete and steel reinforcement. Furthermore, Beam 2 also displays a smaller rate of increase in beam deflection with increasing number of cycles (see Case 2 in Fig. 7). This could be associated with the limited areas where the damage develops and accumulates in the beam, which concentrates mainly over the center span, or for clarity, see Fig. 8b. However, it is interesting to note although the beam exhibits a smaller rate of increase in deflection, the fatigue life of this beam is predicted to last ~700 cycles, which is two orders of magnitude lower than the original life (~60k cycles). This is in general agreement with the reduction in fatigue life seen in severely corroded reinforced concrete beams reported recently by Tanaka *et al.* (2015), although the extent of the reduction in this study is much higher. This could be related to the complete removal of bond from the very beginning and the absence of initial corrosion-related cracking, which can help to dissipate damage and hence have a life prolonging effect.

Overall, the simulation results clearly demonstrate that initial bond removal between the concrete and the steel has significant detrimental effects on fatigue life, in addition to the reduction in post-cracking stiffness as discussed above.

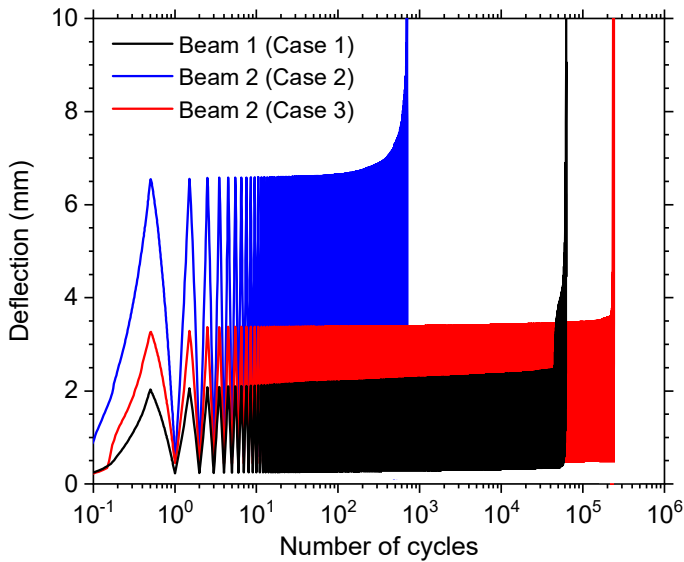


Figure 7. Predicted beam deflection responses under a fixed-point pulsating load.

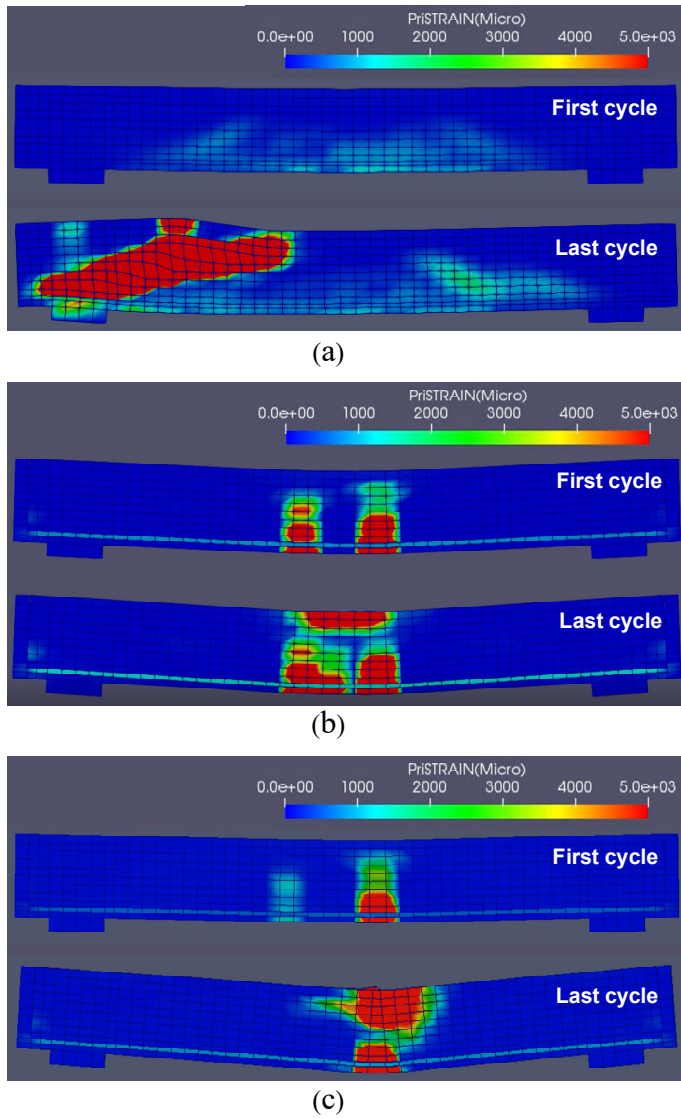


Figure 8. Predicted maximum principal strain contours for (a) Beam 1 subjected to a maximum load of 70% of its load capacity (Analysis Case 1); (b) Beam 2 also to 70% of its load capacity (Analysis Case 2); and (c) Beam 2 to 70% of the original (Beam 1's) load capacity (Analysis Case 3). In all plots, only the principal strains at the maximum applied load are presented.

A further analysis (Analysis Case 3) was undertaken to assess the fatigue life of Beam 2 considering the original load capacity of Beam 1. In other words, no consideration of load capacity enhancement is taken into account (i.e. the maximum applied load is set equal to 70% that of Beam 1, as in Analysis Case 1). This is to simulate the occurrence of a significant bond loss during the lifespan and to check if such a situation would pose a higher risk of fatigue problem. In this study, however, initial cracking is not considered and thus the result could be considered as being conservative.

It is apparent from Figure 7 that Beam 2 (Case 3) still exhibits a larger initial beam deflection and deflection amplitude than Beam 1 and this is once again as a direct result of the reduction in post-cracking stiffness, due to the absence of bond. It is interesting to note that as before, due to the location of damage being limited in small areas over the center span (see Fig. 8c), Beam 2 (Case 3) is predicted to exhibit a smaller rate of increase in beam deflection with increasing number of cycles. Also, from the simulation, it is predicted that Beam 2 would exhibit comparable fatigue life to Beam 1, when the enhancement in load capacity is neglected. Again, this is based on the assumption that the concrete has no initial cracking. Should some initial corrosion-related cracking have been considered, it is expected that the beam would exhibit a longer fatigue life (see, for example, Gebreyouhannes *et al.* (2008)).

Work is currently underway to investigate the fatigue life under different load amplitudes, the influence of non-uniform corrosion and initial cracking, as well as the influence of a more realistic load condition such as moving load.

4 CONCLUDING REMARKS

Nonlinear finite element simulations were carried out to investigate the behaviors of two reinforced concrete beams, one with fully bonded tension reinforcement and the other with non-bonded tension reinforcement, under monotonic and fatigue loading conditions. It is shown that the overall behaviors of the two beams in terms of the load-deflection response, mode of failure, crack pattern and location of failure can be accurately simulated.

The beam containing conventional (fully bonded) tension reinforcement is shown to exhibit a typical flexure-shear response. The simulation shows that the removal of bond throughout the beam span can prevent the occurrence of premature shear failure and hence results in a significant enhancement in load capacity, which confirms the experimental finding. It is shown that bond removal also results in a significant reduction in post-cracking stiffness and accordingly, an increase in beam deflection at the peak load.

The fatigue simulations show that the mode of failure of the two beams under repetitive loading remains unchanged. It is shown that the removal of bond from the initial stage causes a substantial loss of post-cracking stiffness which, in turn, results in a significant increase in initial deflection and deflection amplitude. Damage in the beam is shown to develop over a small region and hence the beam only exhibits a small rate of increase in beam deflection under fatigue loading. However, at 70% of its peak load, the fatigue life of the beam is shown to last two orders of magnitude lower, indicating that complete bond removal has a significant detrimental impact on fatigue life.

The fatigue simulations also show that when the enhancement in load capacity (due to the removal of bond is neglected), the beam is predicted to exhibit a comparable fatigue life, if not longer, despite no consideration of initial cracking. This could be of considerable significance from a practical point of view to suggest that a beam with partial bond loss could have a comparable, if not longer fatigue life. However, it is of importance to ensure that the anchorage of the longitudinal reinforcement at the support remains fully intact, as otherwise it can lead to a premature shear failure (Chijiwa *et al.* 2011).

5 REFERENCES

- Bugalia, N. & Maekawa, K. 2017. Time-dependent capacity of large scale deep beams under sustained loads. *Journal of Advanced Concrete Technology*, 15(7): 314-327.
- Biswas, R.K., Iwanami, M., Chijiwa, N. and Uno K., 2020. Effect of non-uniform rebar corrosion on structural performance of RC structures: A numerical and experimental investigation. *Construction and Building Materials* 230: 116908.
- Chijiwa, N., Kawanaka, I. & Maekawa, K. 2011. Effect of strengthening at expected damaging zone of a RC member with damaged anchorage. *Journal of Japan Society of Civil Engineers E2 (Materials and Concrete Structures)* 67(2): 160-165.
- Collins, M.P., Bentz, E.C. & Sherwood, E.G. 2008. Where is shear reinforcement required? Review of research results and design procedures. *ACI Structural Journal* 105(5): 590-600.
- Fujiyama, C. & Maekawa, K. 2011. A computational simulation for the damage mechanism of steel-concrete composite slabs under high cycle fatigue loads. *Journal of Advanced Concrete Technology* 9(2): 193-204.
- Gebreyouhannes, E., Chijiwa, N., Fujiyama, C. & Maekawa, K. 2008. Shear fatigue simulation of RC beams subjected to fixed pulsating and moving loads. *Journal of Advanced Concrete Technology* 6(1): 215-226.
- Hung, N.H.Q., Komatsu, S. & Maekawa, K. 2019. High-cycle fatigue interaction between soil foundation and concrete slab under moving wheel-type loads. *Engineering Structures* 109931.
- Ikeda, S. & Uji, K. 1980, January. Studies on the effect of bond on the shear behavior of reinforced concrete beams. *Proceedings of the Japan Society of Civil Engineers* 293: 101-109.
- Kotsovos, G.M., Vougioukas, E. & Kotsovos, M.D. 2015. Behaviour of reinforced concrete beams with non-bonded flexural reinforcement. *Magazine of Concrete Research* 67(10): 503-512.
- Maekawa, K., Okamura, H. & Pimanmas A. 2003. *Nonlinear mechanics of Reinforced Concrete*. London: Spon Press.
- Maekawa, K., Toongoenthong, K., Gebreyouhannes, E. & Kishi, T. 2006a. Direct path-integral scheme for fatigue simulation of reinforced concrete in shear. *Journal of Advanced Concrete Technology* 4(1): 159-177.
- Maekawa, K., Gebreyouhannes, E., Mishima, T. & An, X. 2006b. Three-dimensional fatigue simulation of RC slabs under traveling wheel-type loads. *Journal of Advanced Concrete Technology*, 4(3), pp.445-457.
- Maekawa, K., Fukuura, N. & Soltani, M. 2008a. Path-dependent high cycle fatigue modeling of joint interfaces in structural concrete. *Journal of Advanced Concrete Technology* 6(1): 227-242.
- Maekawa, K., Ishida, T. & Kishi T. 2008. *Multi-Scale Modeling of Structural Concrete*. Abingdon: Taylor & Francis.
- Matsuo, T., Sakai, M., Matsumura, T. & Kanazu T. 2004. An Experimental study on shear resisting mechanism of RC beams with corroded reinforcement. *Concrete Research and Technology* 15(2): 69-77.
- Saifullah, H.A., Nakarai, K., Piseth, V., Chijiwa, N. & Maekawa, K. 2017. Shear creep failures of reinforced concrete slender beams without shear reinforcement. *ACI Structural Journal* 114(6): 1581-1590.
- Satoh, Y. 2003. Shear behavior of RC member with corroded shear and longitudinal reinforcing steels. *Proceedings of the Japan Concrete Institute* 25(1): 821-826.
- Suryanto, B., Tambusay, A. & Suprobo, P. 2017. Crack mapping on shear-critical reinforced concrete beams using an open source digital image correlation software. *Civil Engineering Dimension* 19(2): 93-98.
- Suryanto, B. & Staniforth, G. 2019. Monitoring the shear fatigue response of reinforced concrete beams subjected to moving loads using digital image correlation. *Civil Engineering Dimension* 21(1): 6-12.
- Tanaka, Y., Takahasi, Y. & Maekawa, K. 2015. Computational fatigue life assessment of corroded reinforced concrete beams. In C. Hellmich, B. Pichler & J. Kollegger (eds), *Mechanics and Physics of Creep, Shrinkage, and Durability of Concrete and Concrete Structures* 1308-1315; *Proc. intern. symp., Vienna, 21-23 September 2015*. Reston: ASCE.
- Toongoenthong, K. & Maekawa, K. 2005. Multi-mechanical approach to structural performance assessment of corroded RC member in shear. *Journal of Advanced Concrete Technology* 3(1): 107-122.
- Ueda, T. & Okamura, H. 1982. Fatigue behavior of reinforced concrete beams under shear force. *IABSE Colloquium*: 415-422. Lausanne.
- Yamada, Y., Chijiwa, N. & Iwanami, M. 2018. Effect of stirrups on shear fatigue load carrying mechanism of RC beams with rebar corrosion cracks. *Journal of Japan Society of Civil Engineers E2 (Materials and Concrete Structures)* 74: 176-191.